Physics Letters B 678 (2009) 181–185

Contents lists available at ScienceDirect

Physics Letters B

www.elsevier.com/locate/physletb

Search for solar axions produced by Primakoff conversion using resonant absorption by ^{169}Tm nuclei

A.V. Derbin *, S.V. Bakhlanov, A.I. Egorov, I.A. Mitropol'sky, V.N. Muratova, D.A. Semenov, E.V. Unzhakov

St.Petersburg Nuclear Physics Institute, Gatchina 188300, Russia

ARTICLE INFO

Article history:
Received 15 January 2009
Received in revised form 21 April 2009
Accepted 6 June 2009
Available online 11 June 2009
Editor: V. Metag

PACS:
14.80.Mz
29.40.Mc
26.65.+t

Keywords:
Solar axion
Low background measurements

ABSTRACT

The search for resonant absorption of the Primakoff solar axions by ^{169}Tm nuclei have been performed. Such an absorption should lead to the excitation of low-lying nuclear energy level: $A + {}^{169}\mathrm{Tm} \to {}^{169}\mathrm{Tm}^* \to {}^{169}\mathrm{Tm} + \gamma$ (8.41 keV). The Si(Li) detector and ^{169}Tm target placed inside the low-background setup were used for that purpose. As a result, a new restriction on the axion–photon coupling and axion mass was obtained: $g_{A\gamma}(\mathrm{GeV}^{-1}) \cdot m_A(\mathrm{eV}) \leqslant 1.36 \times 10^{-5}$ (90% c.l.). In model of hadronic axion this restriction corresponds to the upper limit on axion mass — $m_A \leqslant 191$ eV for 90% c.l.

1. Introduction

The appearance of an axion in theory is connected with the problem of CP-violation in strong interactions. In order to solve this puzzle Peccei and Quinn [1] proposed the concept of the new chiral symmetry $U(1)$. The spontaneous breaking of this symmetry at the energy f_A allows one to compensate CP-violating term of the QCD Lagrangian completely. Weinberg [2] and Wilczek [3] showed that the introduced model should lead to the occurrence of a new pseudoscalar particle. The axion mass m_A appears to be inversely proportional to the f_A value, as well as the effective axion coupling constants with photons ($g_{A\gamma}$), leptons (g_{Ae}), and hadrons (g_{AN}). The model of "standard" or PQWW-axion, where the value of f_A was fixed at the electroweak scale ($f_A \approx \sqrt{2}G_F)^{-1/2}$ has been excluded by the series of experiments with radioactive sources, reactors and accelerators.

Two types of the "invisible" axion models retained the axion in the form required for the solution of CP-violation problem, while suppressing its interaction with matter, since the scale of symmetry breaking f_A appears to be arbitrary in these models and can be extended up to the Planck mass $m_P \approx 10^{19}$ GeV. These are models of "hadronic" or KSVZ axion [4,5] and the GUT or DFSZ axion [6,7].

The axion mass m_A (in eV units) in both models is given in terms of π^0-properties:

$$m_A = \frac{f_\pi m_\pi}{f_A}\left(\frac{z}{(1+z+w)(1+z)}\right)^{1/2} \approx \frac{6.0\times 10^6}{f_A(\mathrm{GeV})} \tag{1}$$

where $f_\pi \cong 93$ MeV is the pion decay constant; $z = m_u/m_d \cong 0.56$ and $w = m_u/m_s \cong 0.029$ are quark-mass ratios.[1]

The restrictions on the axion mass appear as a result of the restrictions on the coupling constants $g_{A\gamma}$, g_{Ae} and g_{AN}, which are significantly model dependent. The hadronic axion does not interact with leptons and ordinary quarks at the tree level, which results in strong suppression of g_{Ae} coupling through radiatively induced coupling. Moreover, in some models axion–photon coupling may significantly differ from the original DFSZ or KVSZ $g_{A\gamma}$ couplings. The coupling constant $g_{A\gamma}$ for the "invisible" axion models is equal to:

$$g_{A\gamma} = \frac{\alpha}{2\pi f_A}\left(\frac{E}{N} - \frac{2(4+z)}{3(1+z)}\right) = \frac{\alpha}{2\pi f_A}C_{A\gamma} \tag{2}$$

where $\alpha \approx 1/137$ is a fine structure constant, E/N is the ratio of the electromagnetic and colour anomalies, a model dependent parameter is of the order of unity. $E/N = 8/3$ for the DFSZ-axion

* Corresponding author.
E-mail address: derbin@pnpi.spb.ru (A.V. Derbin).

[1] We follow the generally accepted units: GeV for f_A and $g_{A\gamma}$ and eV for m_A.

0370-2693/$ – see front matter
doi:10.1016/j.physletb.2009.06.016

($C_{A\gamma\gamma} = 0.74$) and $E/N = 0$ ($C_{A\gamma\gamma} = -1.92$) in the original KSVZ-axion model. The value of the second term inside brackets is 1.95 ± 0.08 and axion–photon coupling may be reduced by a factor less than 10^{-2} in axion models in which E/N is close to 2 [8].

If axions do exist, then the Sun should be an intense source of these particles. Axions can be efficiently produced in the Sun by the Primakoff conversion of photons in the electric field of the plasma. The resulting axion flux depends on $g^2_{A\gamma}$ and can be detected by inverse Primakoff conversion of axions to photons in laboratory magnetic fields [9–18] or by the coherent conversion to photons in the crystal detectors [19–22]. The expected count rate of photons depends on the axion–photon coupling as $g^4_{A\gamma}$.

In this Letter we present the results of the search for solar axions using the other reaction — the resonant absorption by nuclear target. The γ-rays and conversion electrons produced by the de-excitation of the nuclear level can be registered. The detection probability of the axions is determined by the product $g^2_{A\gamma} \cdot g^2_{AN}$ which is preferable for small $g_{A\gamma}$ values.

There are two other possible mechanisms of axion production in the Sun: the reactions of solar cycle and the excitation of the low-lying energy levels of some nuclei by the high solar temperature. The attempts to detect the resonant absorption of quasi-monochromatic axions emitted in nuclear magnetic transitions were performed in [23–31]. Astrophysical and cosmological data provide restrictive constraints on axion mass so that acceptable m_a values belong to the 10^{-4}–10^{-2} eV region [32,33]. The results of laboratory searches for the axion as well as the astrophysical axion bounds one can find in [33,34].

2. The rate of solar axions absorption by ^{169}Tm nucleus

The energy spectrum of solar axions produced by Primakoff effect is parameterized by the following expression [11,17,35]:

$$\frac{d\Phi_A}{dE_A} = (g_{A\gamma})^2 \cdot 3.82 \times 10^{30} \frac{(E_A)^3}{\exp(E_A/1.103) - 1}, \tag{3}$$

where the value of flux is given in ($\mathrm{cm}^{-2}\,\mathrm{s}^{-1}\,\mathrm{keV}^{-1}$) units, value of E_A energy is given in keV units and the value of $g_{A\gamma}$ is given in GeV^{-1} units. The axion spectrum calculated in assumption that $g_{A\gamma} = 10^{-10}$ GeV^{-1} is given in Fig. 1. The average energy of axions is ≈ 4 keV, but their flux becomes negligibly small at the energies above 15 keV.

As a pseudoscalar particle, the axion should be subject to resonant absorption and emission in the nuclear transitions of a magnetic type. For our experiment we have chosen the ^{169}Tm nucleus as a target. The energy of the first nuclear level ($3/2^+$) is equal to 8.41 keV, the axion flux at this energy is only 7 times less than the maximum level (Fig. 1). The 8.41 keV nuclear level discharges through $M1$-type transition with $E2$-transition admixture value of $\delta^2 = 0.11\%$. Considering the electron conversion ratio $e/\gamma = 263$ [36] one obtains the relative probability of γ-ray emission $\eta = 1/(1 + e/\gamma) = 3.79 \times 10^{-3}$.

The cross-section for the resonant absorption of the axions with the energy E_A is given by the expression that is similar to the one for γ-ray resonant absorption, but the ratio of the nuclear transition probability with the emission of an axion (ω_A) to the probability of magnetic type transition (ω_γ) have to be taken into account. The rate of solar axion absorption by ^{169}Tm nucleus will be

$$R_A = \pi \sigma_{0\gamma} \Gamma \frac{d\Phi_A}{dE_A}(E_A = 8.4)\left(\frac{\omega_A}{\omega_\gamma}\right), \tag{4}$$

where $\sigma_{0\gamma}$ is a maximum cross-section of γ-ray absorption. The experimentally derived value of $\sigma_{0\gamma}$ for ^{169}Tm nucleus is equal

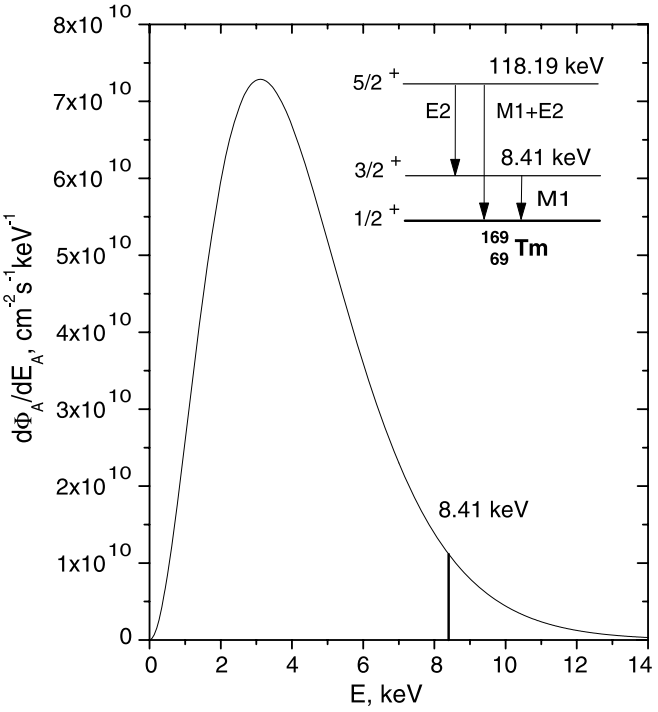

Fig. 1. Energy spectrum of the axions produced by Primakoff effect at the Sun (for $g_{A\gamma} = 10^{-10}$ GeV). The level scheme of ^{169}Tm nucleus is shown in the inset.

to $\sigma_{0\gamma} = 2.56 \times 10^{-19}$ cm^2. A lifetime of the ^{169}Tm first excited level is $\tau = 5.89$ ns, thus the width of the energy level $\Gamma = 1.13 \times 10^{-7}$ eV.

The ω_A/ω_γ ratio calculated in the long-wave approximation, has the following view [37,38]:

$$\frac{\omega_A}{\omega_\gamma} = \frac{1}{2\pi\alpha}\frac{1}{1+\delta^2}\left[\frac{g^0_{AN}\beta + g^3_{AN}}{(\mu_0 - 0.5)\beta + \mu_3 - \eta}\right]^2 \left(\frac{p_A}{p_\gamma}\right)^3. \tag{5}$$

Here, p_γ and p_A are the photon and axion momenta, respectively, $\mu_0 = \mu_p + \mu_n \approx 0.88$ and $\mu_3 = \mu_p - \mu_n \approx 4.71$ are isoscalar and isovector nuclear magnetic momenta, β and η are parameters depending on the particular nuclear matrix elements [38,39]. In case of the ^{169}Tm nucleus, which has the odd number of nucleons and an unpaired proton, in the one-particle approximation the values of β and η can be estimated as $\beta \approx 1.0$ and $\eta \approx 0.5$. For the given parameters the branching ratio can be rewritten as:

$$\frac{\omega_A}{\omega_\gamma} = 1.03\left(g^0_{AN} + g^3_{AN}\right)^2 (p_A/p_\gamma)^3. \tag{6}$$

In the KSVZ axion model the dimensionless isoscalar and isovector coupling constants g^0_{AN} and g^3_{AN} are related to f_A by expressions [8,40]:

$$g^0_{AN} = -\frac{m_N}{6 f_A}\left[2S + (3F - D)\frac{1 + z - 2w}{1 + z + w}\right] \tag{7}$$

and

$$g^3_{AN} = -\frac{m_N}{2 f_A}\left[(D + F)\frac{1 - z}{1 + z + w}\right] \tag{8}$$

where $m_N \approx 939$ MeV is the nucleon mass. The axial-coupling parameters F and D are obtained from hyperon semi-leptonic decays with a high degree of precision: $F = 0.462 \pm 0.011$, $D = 0.808 \pm 0.006$ [41]. The parameter S characterizing the flavor singlet coupling still remains a poorly constrained one. Its value varies from $S = 0.68$ in the naive quark model down to $S = -0.09$

which is given on the basis of the EMC collaboration measurements [42]. The more stringent boundaries ($0.37 \leqslant S \leqslant 0.53$) and ($0.15 \leqslant S \leqslant 0.5$) were found in [43] and [44], accordingly. As a result the value of the sum $(g^0_{AN} + g^3_{AN})$ is determined within a factor of two, but the ratio ω_A/ω_γ does not vanish for any value of parameter S, in the case of the transition caused predominantly by the proton ($\beta \geqslant 0$). We will use $S = 0.5$ as reference when we calculate an axion flux for KSVZ axion model.

The values of g^0_{AN} and g^3_{AN} for the DFSZ axion depend on an additional unknown parameter $\cos^2\beta$ which is defined by the ratio of the Higgs vacuum expectation values. In case of ^{169}Tm $M1$-transition the value of $(\omega_A/\omega_\gamma)^{\mathrm{DFSZ}}$ ratio lies within the interval $\sim (0.1\text{–}2.0)(\omega_A/\omega_\gamma)^{\mathrm{KSVZ}}$. The lower and upper bounds of this interval are defined by values $\cos\beta = 0, 1$, respectively.

In accordance with (3) and (6), the rate of axion absorption by ^{169}Tm nucleus (4) dependent only on the coupling constants is (the model-independent view):

$$R_A = 104 \cdot g^2_{A\gamma}\left(g^0_{AN} + g^3_{AN}\right)^2 (p_A/p_\gamma)^3. \tag{9}$$

Using the relations between g^0_{AN}, g^3_{AN} and axion mass given by KVSZ model (7), the absorption rate can be presented as a function of $g_{A\gamma}$ and axion mass m_A:

$$R_A = 4.80 \times 10^{-13} g^2_{A\gamma} m^2_A (p_A/p_\gamma)^3. \tag{10}$$

At last, one can use the connection between $g_{A\gamma}$ and m_A given by expressions (1) and (2), thus the R_A value appears to be proportional to m^4_A:

$$R_A = 6.64 \times 10^{-32} m^4_A (p_A/p_\gamma)^3. \tag{11}$$

The amount of observed γ-rays that follow the axion absorption depends on the number of target nuclei, measurement time and detector efficiency, while the probability of 8.4 keV peak observation is determined by the background level of the experimental setup.

3. Experimental setup

In order to register 8.41 keV γ-rays we used the planar Si(Li) detector with the diameter of the sensitive region $d \approx 17$ mm and 2.5 mm thick. The detector was mounted inside a vertical vacuum cryostat ≈ 3 mm below the 20 μm thick beryllium window. The Tm_2O_3 target consisting of 306 mg of ^{169}Tm with the diameter of 25 mm ($\rho = 31$ mg/cm^2) was placed directly on the beryllium window. The tantalum collimator of 8-mm radius was situated between the beryllium window and detector surface to exclude events at the boundary of the sensitive volume.

The cryostat was enclosed within the concentric copper (Ø29 cm) and lead (Ø34 cm) shells, which provided the shielding against external radioactivity. The setup was located on the ground surface and was assembled of five $50 \times 50 \times 12$ cm^3 plastic scintillators against the cosmic rays and fast neutrons. The rate of 50 μs veto signals was 600 counts/s, that leads to $\approx 3\%$ dead time. The spectrum of the Si(Li) signals obtained in the coincidence with veto signals allows to check the probability of excitation of the 8.41 keV level by the nuclear active component and cosmic ray muons.

The data-acquisition system of the Si(Li) detector was organized in the following way: the output of the Si(Li) detector was fed to the charge-sensitive preamplifier and then to two separate shaping amplifiers with different gain ratios, which makes it possible to collect spectra from both lower (0–60 keV) and higher (0–500 keV) energy regions. This feature allowed us to monitor the background level over a wide range of natural radioactivity and, in particular, to detect the γ-rays corresponding to the de-excitation of the second

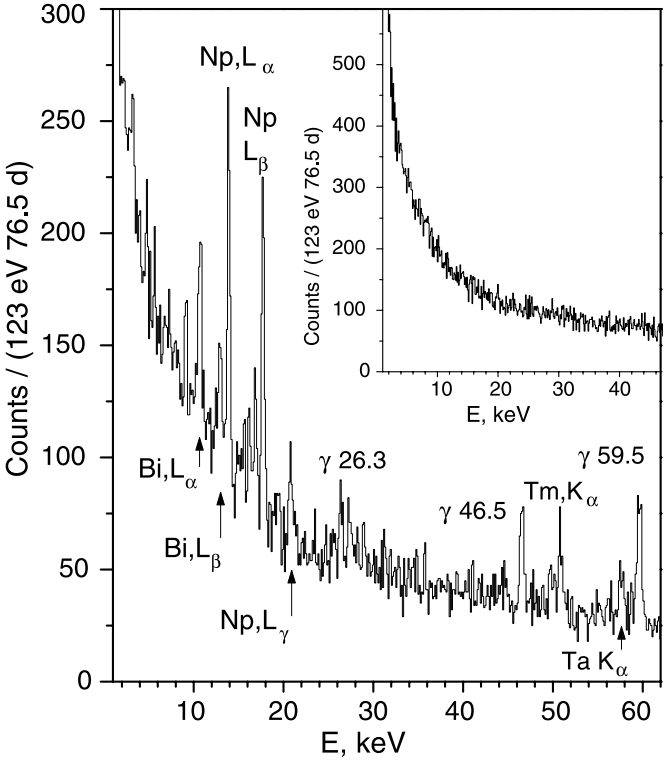

Fig. 2. The Si(Li)-detector spectra measured during 76.5 days: in the anticoincidence (main) and in coincidence (inset) with signal of veto system.

exited state of ^{169}Tm (118 keV). In such a way we can evaluate the fast neutron flux which can excite 8.41 keV level. The signal from each amplifier was received by the individual 4096-channel ADC. Taking into account the spectra measured in coincidence with the veto system for each amplifier, four 4096-channel spectra were recorded.

The energy scale was defined using standard calibration sources of ^{55}Fe, ^{57}Co and ^{241}Am. The prompt energy resolution of the detector determined by the 14.4 keV γ-line from ^{57}Co turned out to be σ = FWHM/2.35 = 120 eV. The high energy resolution and accurate knowledge of the energy scale is very important because the energies of the characteristic X-rays of thulium are very close to 8.41 keV. The most intense L-lines in the case of vacancy on K-shell possesses the following energies and intensities: 7.18 keV (8.1%, $L_{\alpha 1}$), 8.10 keV (5.2%, $L_{\beta 1}$) and 8.47 keV (1.6%, $L_{\beta 2}$).

The sensitive volume and the area of Si(Li) detector were measured using the X-rays from ^{241}Am and ^{55}Tm sources. The self-absorption of 8.41 keV γ-rays by the target was found via a detailed M–C simulation. The results of simulation were tested with ^{241}Am source placed behind the Tm_2O_3 target. The overall detection efficiency for 8.41 keV γ is estimated to be $(1.28 \pm 0.06)\%$.

4. Results

The measurements were carried out during 76.5 days of live time by brief 2-hour runs in order to monitor the time stability of the data-acquisition system. The obtained energy spectra of the Si(Li) detector in the range (1–62) keV are shown in Fig. 2. While the spectrum measured in the coincidence with signals of the veto scintillators does not contain any peculiarity, one can clearly identify several peaks in the spectrum of uncorrelated events.

Two intense peaks with the energies 13.95 keV and 17.8 keV are L X-rays of neptunium that is produced in the ^{241}Am α-decay: $^{241}\mathrm{Am} \rightarrow {}^{237}\mathrm{Np}$. The 13.9 keV peak consists of two lines with the

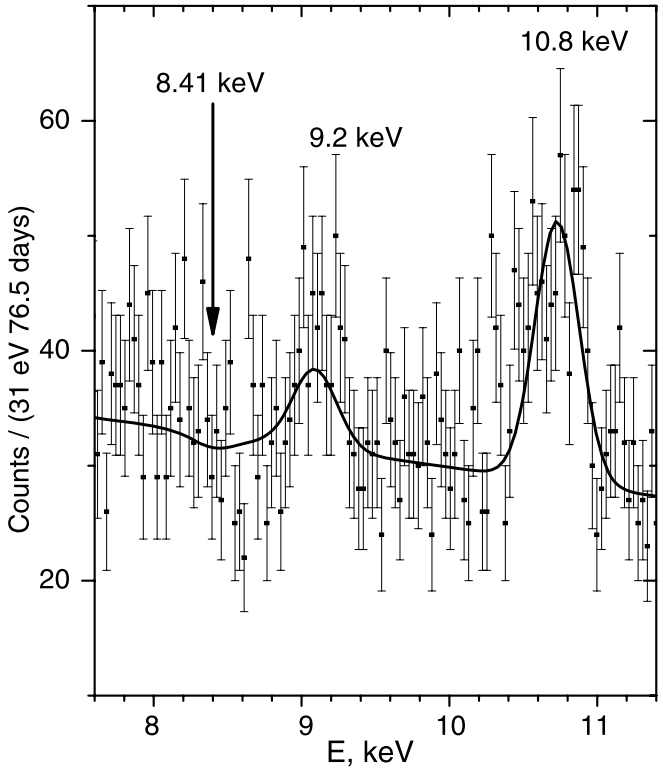

Fig. 3. Energy spectrum measured with the Si(Li)-detector in the region 7.6-11.4 keV. The fit is shown by solid line.

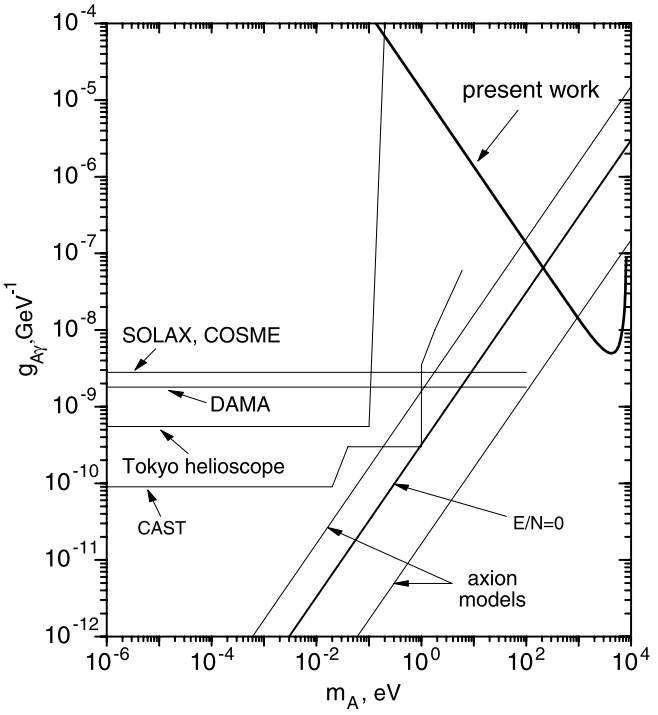

Fig. 4. The limits on $g_{A\gamma}$ coupling constant obtained by Solax [19], Cosme [21], DAMA [20], Tokyo helioscope [16] and CAST [18] experiments. The areas of excluded values are located above the corresponding lines.

energies 13.946 keV (13%, $L_{\alpha 1}$) and 13.761 (1.4%, $L_{\alpha 2}$), the 17.8 keV peak is more complex one formed by $L_{\beta 1-5}$ lines. The less intense peaks with energies of 10.84 keV and 13.2 keV ($L_{\alpha 1}$ and $L_{\beta(1-5)}$ of Bi, respectively) are present due to $^{210}\mathrm{Pb} \to {}^{210}\mathrm{Bi}$ β-decay in ^{238}U series. The well known 59.54 keV ^{241}Am and 46.54 keV ^{210}Pb γ-lines, as well as 50.7 keV $K_{\alpha 1}$ of Tm and 57.5 keV $K_{\alpha 1}$ of Ta X-rays, were observed in the high energy part of the spectrum. The 13.9 keV peak together with 46.54 keV and 59.54 keV γ-peaks were used to find the final energy scale and the energy resolution $\sigma(E)$ of the detector. Since no special electronic stabilization was used, the energy resolution determined for the 13.9 keV peak ($L_{\alpha 1}$ of Np with small admixture of $L_{\alpha 2}$) spread up to $\sigma \cong 130$ eV during the long-time measurements.

Fig. 3 shows the detailed energy spectrum within the (7.6–11.4) keV interval, where the "axion peak" was expected. There is no pronounced peak at 8.41 keV. In order to determine the intensity of the 8.41 keV peak we used the maximum likelihood method. The likelihood function was determined as a sum of three Gaussians and the linear background assuming that the number of counts in each channel had normal distribution. The first Gaussian represents the known characteristic $L_{\alpha 1}$ X-rays of Bi ($E_1 \cong 10.8$ keV, the second Gaussian describes the shape of the peak with the energy $E_2 \cong 9.2$ keV, that we explain by $L_{\alpha 1}$ X-rays of Ir ($L_{\beta 1}$ 10.72 keV X-rays of Ir spread 10.8 keV peak) and the third Gaussian (S_A) stands for the expected 8.41 keV axion peak:

$$N(E) = a + b \cdot E + \frac{1}{\sqrt{2\pi}\sigma} \sum_{i=1}^{3} S_i \exp\left[-\frac{(E_i - E)^2}{2\sigma^2}\right]. \tag{12}$$

The energy resolution (σ) and the position of 8.41 peak was fixed during the fitting, while the positions (E_1, E_2) and intensities (S_1, S_2, S_A) and background coefficients (a,b) were independent free parameters.

The fitting result is given in Fig. 3 (solid line). The minimum of $\chi^2/n.d.f = 121.9/115$ corresponds to the nonphysical value of the axion peak area $S_A = -14$ events. The upper limit on the number of events within the peak was found via a conventional approach: the dependence of χ^2 on the peak area S_A was calculated for various values of S_A while the rest of the parameters were free. Then the appearance probability of the given $\chi^2(S_A)$ value was found and the obtained function $P(\chi^2(S_A))$ was normalized to unity for the $S_A \geqslant 0$ region. The upper limit appeared to be equal to $S_{\lim} = 31$ events for 90% c.l.

For the given rate of axion absorption R_A the expected number of registered 8.41 keV γ-quanta is:

$$S_A = \varepsilon \cdot \eta \cdot N_{169Tm} \cdot T \cdot R_A = 3.49 \times 10^{23} \cdot R_A \leqslant S_{\lim}, \tag{13}$$

where $N_{169Tm} = 1.09 \times 10^{21}$ – the number of ^{169}Tm nuclei, $T = 6.61 \times 10^6$ s – time of measurement, $\varepsilon = 1.28 \times 10^{-2}$ – detection efficiency and $\eta = 3.79 \times 10^{-3}$ – internal conversion ratio.

The relation (13) obtained in the experiment ($R_A \leqslant 8.8 \times 10^{-23}$) limits the region of possible values of the coupling constant $g_{A\gamma}$, g^0_{AN}, g^3_{AN} and axion mass m_A. In accordance with Eqs. (9), (10), (11) and on condition that $(p_A/p_\gamma)^3 \cong 1$ provided for $m_A < 2$ keV one can obtain:

$$g_{A\gamma} \cdot \left|\left(g^0_{AN} + g^3_{AN}\right)\right| \leqslant 9.2 \times 10^{-13}, \tag{14}$$

$$g_{A\gamma}\left(\mathrm{GeV}^{-1}\right) \cdot m_A(\mathrm{eV}) \leqslant 1.36 \times 10^{-5}, \tag{15}$$

$$m_A \leqslant 191 \text{ eV}, \tag{16}$$

all at 90% c.l.

The limit (14) is a model independent one on axion–photon and axion–nucleon couplings. The result (15) (the dimensionless quantity $g_{A\gamma} m_A \leqslant 1.36 \times 10^{-14}$) presented asa restriction on the

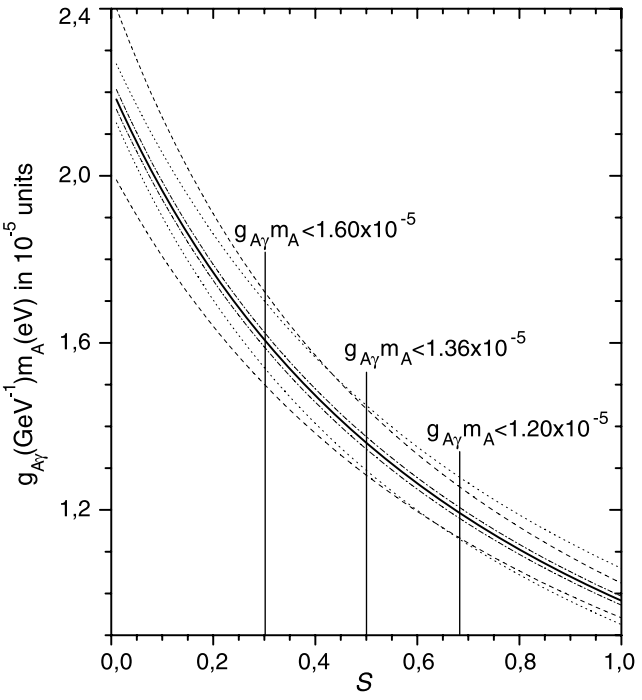

Fig. 5. The limit on $g_{A\gamma}(\mathrm{GeV}^{-1})\cdot m_A(\mathrm{eV}^{-1})$ versus the value of S parameter ($\beta = 1$, $\eta = 0.5$, $z = 0.56$, solid line). The doted, dash-doted and dashed lines correspond to the values of β, η and z changed on $\pm 10\%$, correspondingly.

range of possible values of $g_{A\gamma}$ and m_A (extracted from g_{AN}) allows us to compare our result with the results of experiments using the conversion of axions to photon in the laboratory magnetic field or in the field of crystals [9–21]. The comparisons are shown in Fig. 4. One can see that our results exclude a region of relatively large values of $g_{A\gamma}$ and m_A. For $m_A \approx 1$ keV the limit on the $g_{A\gamma} \approx 10^{-8}$ GeV^{-8} is only several times lower than obtained for low axion masses.

The limit on the hadronic axion mass ($m_A \leqslant 191$ eV), obtained with the new method, is the strongest one up to date among the results of axion detection experiments based on the resonant absorption of monochromatic axions [24–31] or axio-electric effect [45,46]. The obtained limit depends on the exact values of the parameters S, β, η and z. As mentioned above and in contrast with the 14.4 keV ^{57}Fe solar axions [39], the uncertainty of the flavor-singlet axial-vector matrix element S does not change the obtained constraints significantly: $m_A \leqslant 210$ eV ($S = 0.3$) and $m_A \leqslant 180$ eV ($S = 0.7$). The changes of the nuclear-structure dependent terms β from 0.5 to 1.5 and η from -1 to $+1$ lead to the limits $m_A \leqslant$ (223–158) eV and $m_A \leqslant$ (220–180) eV, correspondingly. The usually accepted value of u- and d-quark-mass ratio ($z = 0.56$) can vary in the range 0.35–0.6 [33], in this case our obtained results become $m_A \leqslant$ (161–196) eV. The dependencies of the limits on $g_{A\gamma}m_A$ vs S for the various values of β, η and z are given in Fig. 5.

The sensitivity of the experiment depends on the total efficiency of registration defined by the product $\eta \cdot \epsilon$ which is $\approx 5 \times 10^{-5}$ in our case. This value can be increased significantly by introducing the Tm target inside the volume of a scintillator.

5. Conclusion

The search for the resonant absorption of solar axions produced by Primakoff conversion was performed. For that purpose we used the low-background setup consisting of Si(Li)-detector, ^{169}Tm target, active and passive shielding. The obtained upper limit on the values of the coupling constant and the axion mass is $g_{A\gamma}(\mathrm{GeV}^{-1})\cdot m_A(\mathrm{eV}) \leqslant 1.36 \times 10^{-5}$, which allowed us to set the upper limit on hadronic axion mass $m_A \leqslant 191$ eV (90% C.L.) ($S = 0.5$).

Acknowledgements

The work of E.V. Unzhakov was supported by a grant of Saint-Petersburg Government, project No. 2.4/29-04/17.

References

[1] R.D. Peccei, H.R. Quinn, Phys. Rev. Lett. 38 (1977) 1440.
[2] S. Weinberg, Phys. Rev. Lett. 40 (1978) 223.
[3] F. Wilczek, Phys. Rev. Lett. 40 (1978) 279.
[4] J.E. Kim, Phys. Rev. Lett. 43 (1979) 103.
[5] M.A. Shifman, A.I. Vainstein, V.I. Zakharov, Nucl. Phys. B 166 (1980) 493.
[6] A.R. Zhitnitskii, Yad. Fiz. 31 (1980) 497, Sov. J. Nucl. Phys. 31 (1980) 260.
[7] M. Dine, F. Fischler, M. Srednicki, Phys. Lett. B 104 (1981) 199.
[8] D.B. Kaplan, Nucl. Phys. B 260 (1985) 215.
[9] P. Sikivie, Phys. Rev. Lett. 51 (1983) 1415;
P. Sikivie, Phys. Rev. D 32 (1985) 2988.
[10] L. Krauss, et al., Phys. Rev. Lett. 55 (1987) 1797.
[11] K. van Bibber, et al., Phys. Rev. D 39 (1989) 2089.
[12] W. Wuensch, et al., Phys. Rev. D 40 (1989) 3153.
[13] C. Hagmann, et al., Phys. Rev. Lett. 80 (1998) 2043.
[14] M. Muck, J.B. Kycia, J. Clarke, Appl. Phys. Lett. 78 (2001) 967.
[15] D. Lazarus, et al., Phys. Rev. Lett. 69 (1992) 2333.
[16] Y. Inoue, et al., Phys. Lett. B 536 (2002) 18;
Y. Inoue, et al., Phys. Lett. B 668 (2008) 93.
[17] K. Zioutas, et al., CAST Collaboration, Phys. Rev. Lett. 94 (2005) 121301.
[18] E. Arik, et al., CAST Collaboration, JCAP 0902 (2009) 008, arXiv:0810.4482.
[19] F.T. Avignone, et al., Solax Collaboration, Nucl. Phys. B (Proc. Suppl.) 72 (1999) 176.
[20] R. Bernabei, et al., DAMA Collaboration, Phys. Lett. B 515 (2001) 6.
[21] A. Morales, et al., Cosme Collaboration, Astropart. Phys. 16 (2002) 325.
[22] T. Bruch, CDMS Collaboration, arXiv:0811.4171 [astro-ph].
[23] S. Moriyama, Phys. Rev. Lett. 75 (1995) 3222.
[24] M. Krçmar, et al., Phys. Lett. B 442 (1998) 38.
[25] M. Krçmar, et al., Phys. Rev. D 64 (2001) 115016.
[26] K. Jakovçiç, et al., nuclex/0402016.
[27] A.V. Derbin, et al., JETP Lett. 81 (2005) 365.
[28] A.V. Derbin, et al., JETP Lett. 85 (2007) 12.
[29] A.V. Derbin, et al., Bull. Rus. Acad. Sci. Phys. 71 (2007) 832.
[30] T. Namba, Phys. Lett. B 645 (2007) 398.
[31] P. Belli, et al., Nucl. Phys. A 806 (2008) 388.
[32] S. Hannestad, et al., arXiv:0706.9148;
G. Raffelt, et al., arXiv:0808.0814.
[33] C. Amsler, et al., Particle Data Group, Phys. Lett. B 667 (2008) 1.
[34] G.G. Raffelt, arXiv:hep-ph/0611350.
[35] R.J. Creswick, et al., Phys. Lett. B 427 (1998) 235.
[36] Nuclear Data Sheets, $A = 169$, 109 (2008).
[37] T.W. Donnelly, et al., Phys. Rev. D 18 (1978) 1607.
[38] F.T. Avignone III, et al., Phys. Rev. D 37 (1988) 618.
[39] W.C. Haxton, K.Y. Lee, Phys. Rev. Lett. 66 (1991) 2557.
[40] M. Srednicki, Nucl. Phys. B 260 (1985) 689.
[41] V. Mateu, A. Pich, JHEP 0510 (2005) 41.
[42] R. Mayle, et al., Phys. Lett. B 219 (1989).
[43] G. Altarelli, et al., Phys. Lett. B 496 (1997) 337.
[44] D. Adams, et al., Phys. Rev. D 56 (1997) 5330.
[45] A. Ljubicic, et al., Phys. Lett. B 599 (2004) 143.
[46] D. Kekez, et al., arXiv:0807.3482.